Study of temperature fields inside a canarian greenhouse

K. LEKOUCH, M. EL JAZOULI*, L. BOUIRDEN
Laboratory of Thermodynamics and Energy,
Faculty of Sciences, University Ibn zohrcité
Dakhla BP 8106 Agadir, MORROCO.

Abstract: The climatic factors that influence the climate inside the greenhouse are temperature, humidity, solar radiation, wind and plant cover. Temperature is the most important factor in the growth and development of vegetation. Thus, a well controlled temperature allows the physiological development of the plants. This study presents an analysis and simulation of temperature fields in canarian greenhouse equipped with anti-insect nets. The site is located in the coastal area of southern Morocco. The study is carried out during two period daytime and night to determine cooling or heating requirements, with consideration of the long and short wavelength balance and the radiative convective coupling. The fundamental calculation of climatic conditions is based on CFD. The dynamic influence of the insect screens and tomato crop on airflow movement, was described ,using the concept of the porous medium approach proposed by Darcy and Forchheimer. The coupling of convective and radiative exchanges at the plastic roof cover is considered. This CFD study assisted for exploration of inside climate and allows for a better assessment of the overall climate and plant activity. A good agreement was observed between the measured and simulated values for inside temperature. The results clearly showed the heterogeneity of the greenhouse's internal climate, which infects agricultural production in quantity and quality.

Key-words : Canarian Greenhouse; CFD; temperature fields ;Insect screens;

Received: May 23, 2021. Revised: March 21, 2022. Accepted: April 22, 2022. Published: May 24, 2022.

1. Introduction

In south Morocco, the agricultural production is limited by unfavorable climatic conditions, wich penalize the production in quantity and quality. Moreover, the presence of thrips and aphides are responsible for significant crop damage.Therfore,the use of very fine anti-insect proof nets has been recognized to reduce the need for pesticide application. They act as mechanical barriers to insects but olso reduce the ventilation rate,and raise inside temperature and humidity. [1-7]

The studies for the dynamic characterization of these nets have been based on experimental studies. Computational fluid Dynamics (CFD) have been increasingly used to study greenhouse ventilation. The effects of insect screens on ventilation, have been characterized and numerically modelled,in a tunnel greenhouse.The effect of wind speed on natural ventilation have also been analysed in a greenhouse using a three-dimensional and a two-dimentional CFD simulation respectively. [8-15]

The aim of the present study, was to analyse the distribution of temperature fields in a canarian greenhouse installed in southern Morocco, in order to find a structure better adapted to the climatic conditions of our region. It is a commercial greenhouse covered with a plastic cover, It occupies a surface of 11,250 m²and its average height is 5 m. The orientation of the "chapels" is North-South, that is, perpendicular to the direction of the prevailing wind. The ventilation of the greenhouse studied is provided by seventeen openers (0.6x125 m² each, or 1275 m2 in all) and Covered with nets against insects type 20 x 10 (anti-Thrips). The side walls of the greenhouse have fixed-sized openings and are equipped with the same type of nets.

We combined an experimental and modelling study. The numerical climate model is based on (CFD) simulation of sensible and latent heat exchanges between the tomato crop and the greenhouse air, with combination of radiative transfers at roof level. The model was first validated by measured data and then used to explore the details of air flow, temperature. This CFD assisted for exploration of inside climate and allows for a better assessment of the overall climate and plant activity.

2. Theory

We note that the nomenclature with the explanations of all variables can be found at the end of the paper

2.1. aerodynamic equations:

The mass, momentum, energie and concentration equations can be represented with the following conservation equation:.

$$\frac{\partial \Phi}{\partial t}+\frac{\partial}{\partial x_j}(u_j\Phi)=\frac{\partial}{\partial x_j}(\Gamma_\Phi\frac{\partial \Phi}{\partial x_j})+S_\Phi \quad (1)$$

2.2 *Modeling of flow through insect screens and plants :*

The drag forces induced by insect screens and crop, that correspond to the term S_Φ ,is included into our CFD study by the porous medium approach given by the Darcy–Forchheimer equation: [16]

$$S_\Phi = -\left(\frac{\mu}{K}U + \rho\frac{C_f}{\sqrt{K}}U^2\right) \quad (2)$$

$$K = 3.44\times10^{-9}\alpha^{1.6} \quad (3)$$

$$C_f = \frac{4.30\times10^{-2}}{\alpha^{2.13}} \quad (4)$$

α is the screen porosity deduced from the thread dimensions. : [17]

$$\alpha = \frac{L.W}{(L+d)(W+d)} \quad (5)$$

L = 0.788 mm and W= 0.255 mm are respectively meshes length and width,
d = 0.28 mm, is the wire diameter.
For the low air speed (0.1-0.5 $m.s^{-1}$), we can considers only the second member of relation (2):

$$S_\Phi = -\rho\frac{C_f}{\sqrt{K}}U^2 \quad (6)$$

The non-linear momentum loss coefficient C_f and the permeability K can be deduced from equation: [15]

$$\frac{C_f}{\sqrt{K}} = I_{LA}\,C_D \quad (7)$$

The radiative net flux R_{net} reaching each mesh ,is partitioned into convective sensible Q_{sens} and latent heat fluxes Q_{lat}: [15]

$$R_{net} - Q_{sen} - Q_{lat} = 0 \quad (8)$$

The sensible heat flux Q_{sen} was expressed with the temperature difference between inside air and canopy :

$$Q_{sen} = \rho C_p I_{AV}\left(\frac{(T_v - T_i)}{r_a}\right) \quad (9)$$

The aerodynamic resistance r_a was deduced from the air speed:

$$r_a = \frac{\rho C_p}{0.288\lambda}\left(\frac{d_v \upsilon}{U}\right)^{0.5} \quad (10)$$

The latent heat fluxes Q_{lat} was deduced from the humidity difference.

$$Q_{lat} = \rho l_v l_e^{1/3} I_{AV}\left(\frac{w_v^* - w_i}{r_s + r_a}\right) \quad (11)$$

The Tomato leafstomatal resistance r_s was deduced from air temperature and saturation deficit values using Boulard et al.formula:

$$r_s = r_{s\min}\left[1 + 0.11\exp(0.34(6.107.10^{\frac{7.5T_i}{237.5+T_i}} - 1629w_i - D_{\max}))\right] \quad (12)$$

.

The solar radiation received at a height z (m) is expressed by the following equation: : [17]

$$R(z) = R_{gi}\exp(-k_c I_{LAS}(\frac{H-z}{z})) \quad (13)$$

$$R_{abs} = R(z_1) - R(z_2) = dR(z) \quad (14)$$

Finally the tomato crop temperature (T_v) can be calculated according to the following equations:

$$T_v = T_i + \frac{r_a}{\rho C_p}\left[\frac{1}{2I_{LAV}}\frac{dR(z)}{dz} - \rho L_v L_e^{1/3}\frac{(w_i - w_a)}{r_t}\right] \quad (15)$$

3. Materials and methods

3.1. The greenhouse

The studied greenhouse (Fig. 2) is a commercial canarian greenhouse. The greenhouse is covered with a plastic cover, It occupies a surface of 11,250 m²and its average height is 5 m. The orientation of the "chapels" is North-South, that is, perpendicular to the direction of the prevailing wind. The ventilation is provided by seventeen openers arranged in roof (0.6 125 m² each, or 1275 m2 in all) and covered with protective nets against insects of type 20 x 10 (anti-Thrips). The side walls of the greenhouse have fixed-sized openings and are equipped with the same type of nets.

Fig.1 : interior photo of the studied greenhouse .

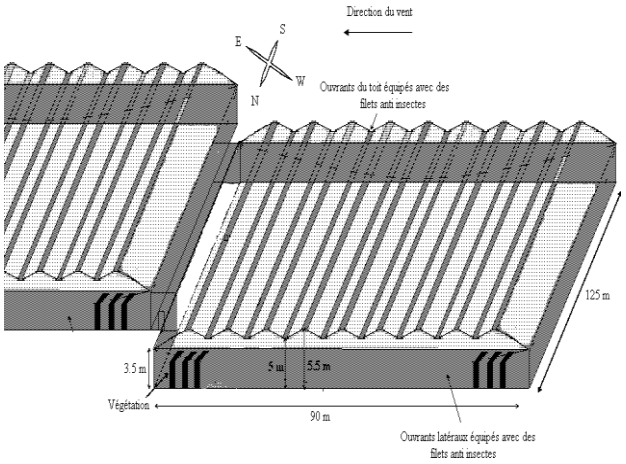

Fig. 2 : Representative scheme of the greenhouse and its ventilation system.

3.2. mesh size and boundary conditions

3.2.1 mesh size

The mesh used in this study is of the BFC type composed of 192, 44 and 112 meshes according to the axes respectively $\vec{x}$, $\vec{y}$, $\vec{z}$ (total 860160). The calculation domain also includes the free space on the windward side (30 m), the downwind sides (30 m) and along both sides (2 x 30 m) of the greenhouse.

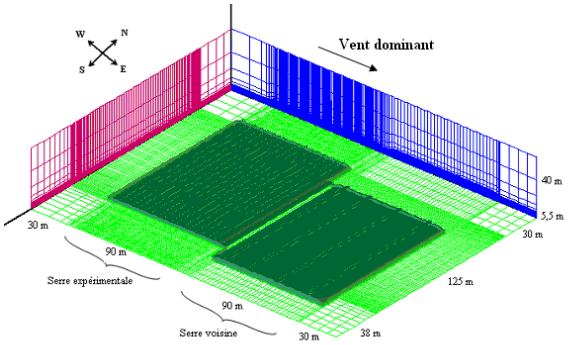

Fig. 3 : Mesh used to simulate the greenhouse .

3.2.2 boundary conditions

The conditions at the outside ground temperature limits of the greenhouse correspond to the averages of the values measured experimentally.
Thermal conditions at the walls : Generally, wall conditions of the «WALL» type are used , however, the side walls have been treated as porous.

4. Results and discussion

4.1. Model validation

Figures 4, 5,6and 7 represent the evolution of the simulated temperature profiles measured in the centre and along the length from west to east, to two different heights: 1 m and 4 m. It is observed that in general, the simulated values are slightly lower than the measured values.

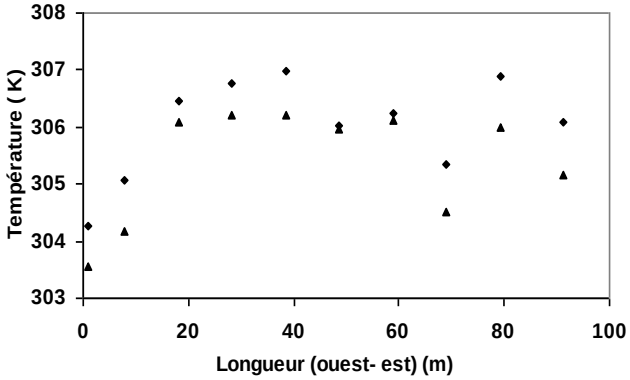

Fig.4: Evolution of daytime temperature profiles simulated and measured at the centre of the greenhouse at 1 m above the ground, depending on the length of the greenhouse (cut in the centre of the greenhouse) measured (♦) simulated (▲)

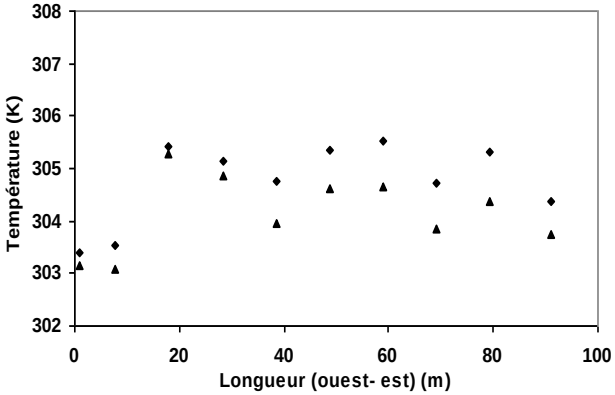

Fig. 5: Evolution of daytime temperature profiles simulated and measured at the centre of the greenhouse at 4 m above the ground, according to the length of the greenhouse (cut in the centre of the greenhouse) measured (♦) simulated (▲)

.

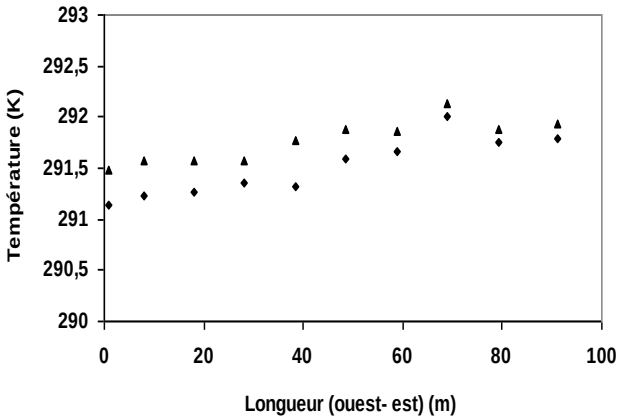

Fig. 6: simulated and measured night temperature profiles at 1 m above ground level as a function of greenhouse length measured (♦) simulated (▲)

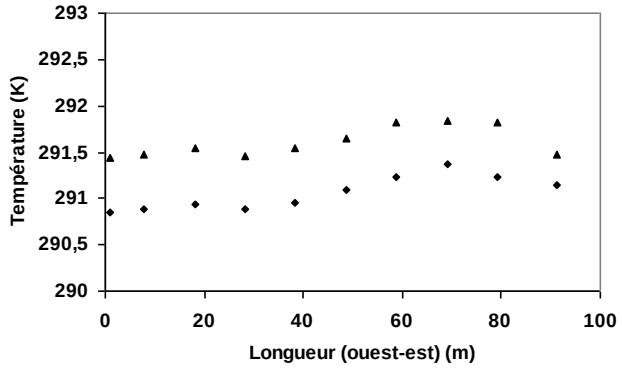

Fig. 7: Evolution of the simulated and measured profiles of the night temperature at 4 m above the ground as a function of the length of the greenhouse measured (♦) simulated (▲)

4.2 Detailed description of the thermal field within the greenhouse

4.2.1 study of diurnal microclimate :

Figures 8,9 and 10 represent respectively the simulated thermal fields in horizontal sections 1, 3 and 4 m above ground level. It is observed that the temperature is high inside the greenhouse and that its distribution depends strongly on the penetration of the outside air which significantly cools the inside air. At the openings 4 m above the ground and above the vegetation the temperature is almost constant, while at the ground level it is heterogeneous. The warmest area (311 K) is at ground level. approximately 12 m downstream from the greenhouse entrance. This is the most critical area of the greenhouse.

At the height of 1 m, there are two distinct zones: Warmer areas are at the junction of the convection cells. This temperature increase particularly at12m downstream of the greenhouse inlet near the windward end where interference between the incoming air current and an internal air current blowing in the opposite direction is observed.

In general, there is significant temperature heterogeneity at this level. This is mainly due to the geometry of the roof and the alternating arrangement of the ventilation openings on the roof in high (5.5 m) and low (5 m) position relative to the prevailing wind direction. This arrangement has a remarkable effect on the circulation of air within the greenhouse. the temperature difference between inside and outside the greenhouse is less than that observed at 1 m, This limitation of heating is explained by the contribution of the roof openings to the ventilation of the area above the vegetation.

Figure 11 shows a vertical section of the air temperature field at the centre of the greenhouse in the direction of flow. This figure shows the very high temperature gradient that develops in areas near the greenhouse cover and the soil. It also shows the existence of the 8 cold air intakes corresponding to the roof ridge openings located in the "low" position at 5 m above the ground and the 9 hot air outlets corresponding to the ridge openings located in the "high" position 5.5 m above ground level .

Figure 12 shows the simulated vertical temperature profile at the centre of the greenhouse as a function of height. It synthesizes the previously reported observations that the temperature is very high at the level of the soil surface, then that it decreases with the height, up to about 4 m. Then we observe a slight increase in temperature which reaches its maximum at the level of the plastic cover. These two temperature peaks are explained by the high absorption of radiation by the PE film and the soil surface.

Figures 13, 14 and 15 represent the temperature profiles at 1, 3 and 4 m above the ground, respectively, as a function of the length of the greenhouse from west to east. It is observed that at 1 m in height, the temperature distribution is very heterogeneous with high values located in the areas below the hot air outlets (309 K) and lower values in areas just below the cold air intakes (306 K). We can also note the same alternations at 3 and 4 m but with a strong damping of the variations compared to those recorded at 1 m.

Figures 16 and 17 represent the temperature profiles at 1 and 4 m above the ground as a function of the width of the greenhouse (North to South), respectively, they highlight the existence of a great homogeneity of the temperature distribution over the width of the greenhouse. This phenomenon is due mainly to the entrance of air

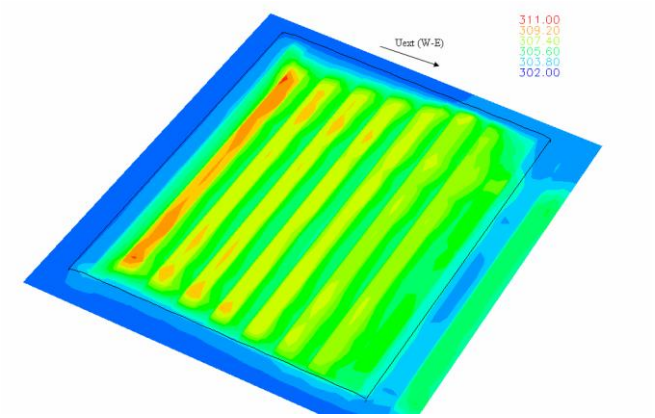

Fig.8:Simulated thermal field
(horizontal cut to 1 m above ground level)

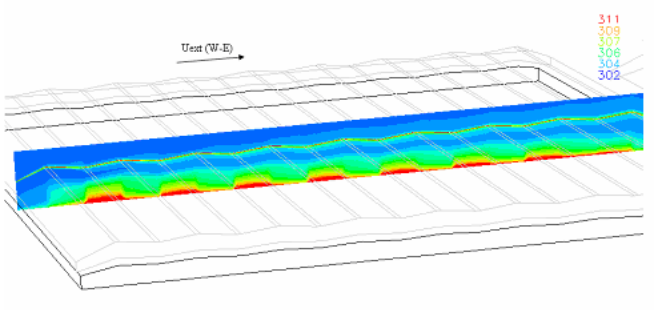

Fig 11 : Simulated thermal field (K) in the centre of the greenhouse
(vertical cut in direction of flow)

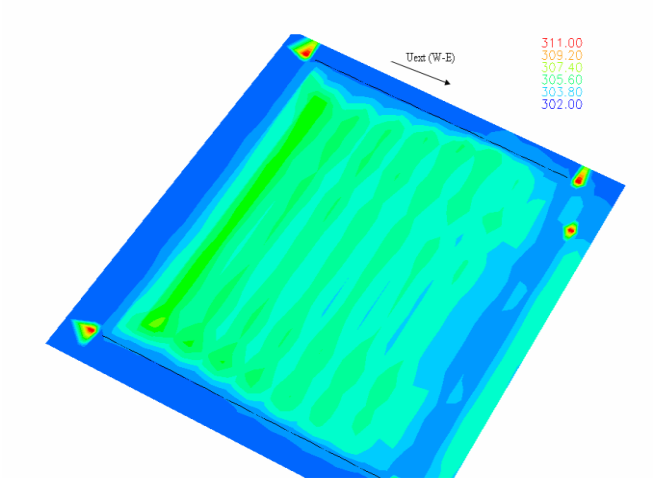

Fig. 9: Simulated thermal field
(horizontal cut 3 m above ground level)

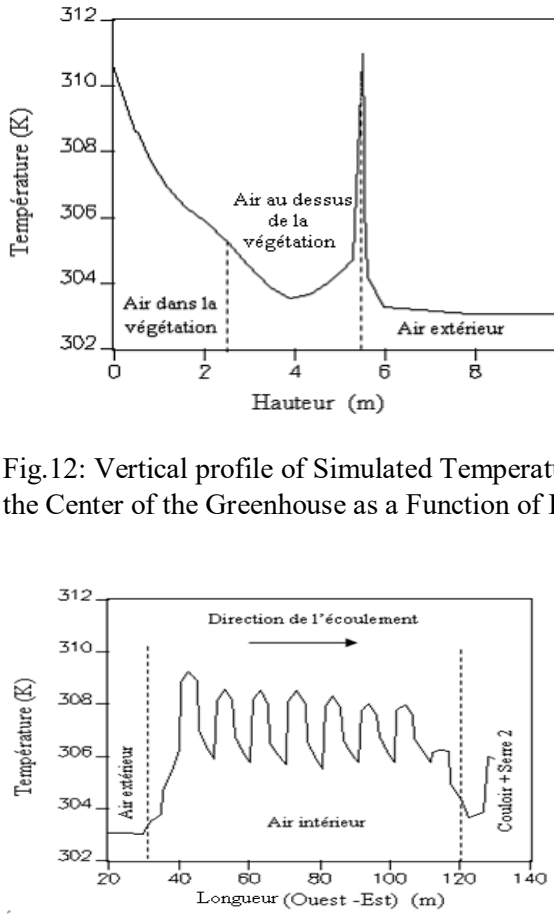

Fig.12: Vertical profile of Simulated Temperature at the Center of the Greenhouse as a Function of Height

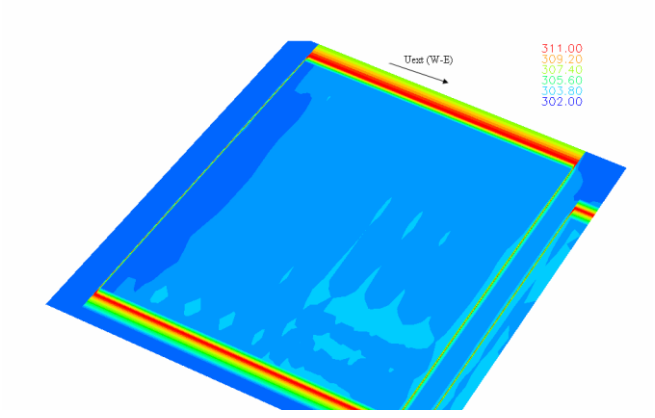

Fig. 10 : Champ thermique simulé
(coupe horizontale à 4 m au-dessus du sol)

Fig. 13:Temperature profile simulated at 1m above the ground depending on the length of the greenhouse**:**

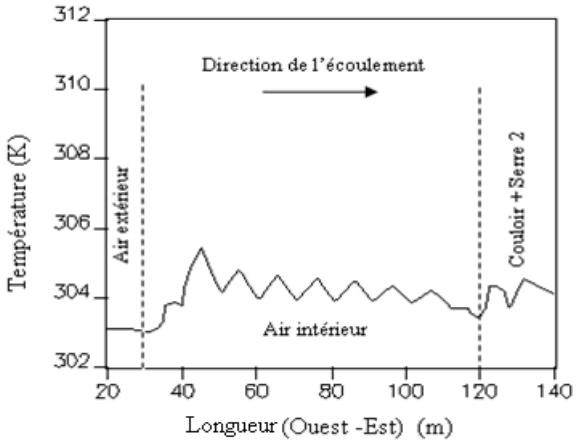

Fig. 14: Temperature profile simulated at 3 m above the ground depending on the length of the greenhouse

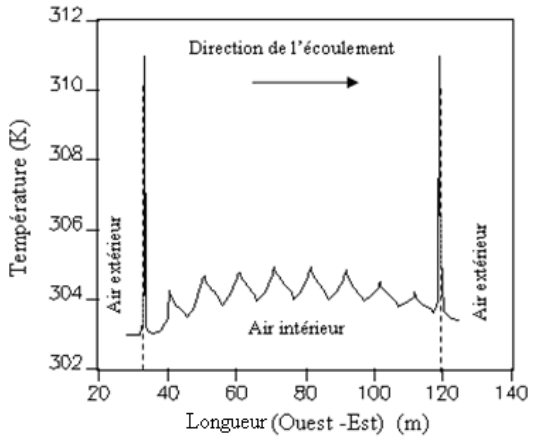

Fig. 15: Temperature profile simulated at 4 m above the ground depending on the length of the greenhouse

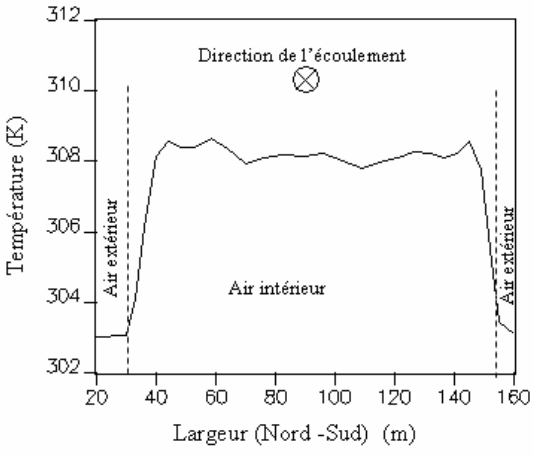

Fig. 16:Simulated temperature profile 1m above the ground depending on the width of the greenhouse

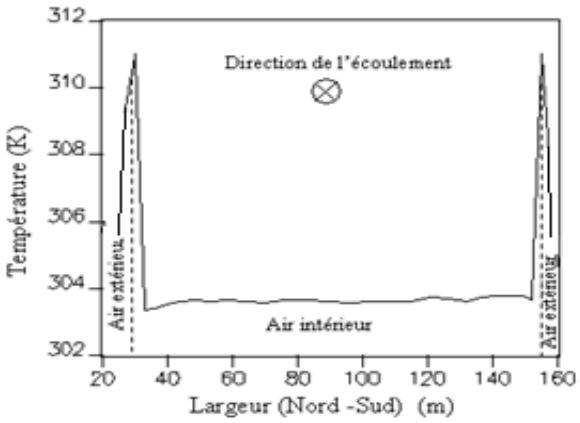

Fig. 17 : Temperature profile simulated at 4m above the ground depending on the width of the greenhouse

4.2.2. Study of Nocturnal Microclimate

For the same geometric configuration (including opening) of the greenhouse previously studied during the daytime, we examined the distribution of its microclimate during the night period. In Table 5.3, the averages and standard deviations of the different climatic parameters used as conditions at the initial limits or conditions for this simulation of the nocturnal microclimate.

Paramètres	Moyenne	Ecart type
External temperature T_e (°C)	29,74	0,95
External relative humidity Rh_e (%)	45,08	2,6
Sky temperature T_{sky} (°C)	17,83	1,15
Vegetation temperature T_v (°C)	35,97	0,36
Greenhouse Soil Surface Temperature T_{si} (°C)	36,67	0,88
wind direction D_v (degré)	125,73	7,45
Wind speed (m/s)	1,3	0,027
Net radiation above vegetation (W/m²)	298,75	2,43
soil flow (W/m²)	50	1,11

Table 1: Experimental (average) measurements taken between 2 and 5 in the morning for 3 days) and used as boundary conditions for night microclimate simulation.

Figures 18 and 19 show the temperature field in a vertical plane at the centre of the greenhouse in parallel and perpendicular sections respectively to the direction of the prevailing wind (West-East). These two figures highlight the existence of an almost perfect homogeneity of the internal temperature of the greenhouse during the night.

With a slight rise in temperature in the vicinity of the ground surface +1.5°C due to the thermal flux imposed by the latter during the night.

The greenhouse roof is approximately 2°C colder than the outside air and 1.5°C colder than the greenhouse air. Figure 20, relating to a horizontal section of the temperature field at 1 m above the ground, shows the almost perfect homogeneity of the distribution temperature within the vegetation. Beyond the height of the canopy (Figure 21) the distribution is more heterogeneous, with a rather small variation.

The analysis in Figure 22, which summarizes the evolution of the temperature profile at the centre of the greenhouse as a function of height, shows that the maximum temperature is found near the surface of the soil. We then observe a slight decrease in temperature within the canopy. Above the canopy the temperature becomes similar to that of the outside.

Figures 23, 24 and 25 represent the evolution of temperature profiles as a function of the length of the greenhouse, moving from west to east over three different heights respectively: 1, 3 and 4 m. These three figures confirm that the temperature above the vegetation (3 and 4 m) is the same as that of the outdoor air, with a slight decrease within the vegetation cover.

Overall, the temperature is perfectly homogeneous for a given height. According to figures 26 and 27, which represent the evolution of temperature profiles as a function of the width of the greenhouse for two different heights (1 and 4 m). We note that this temperature homogeneity for the same height is also true along the North-South axis.

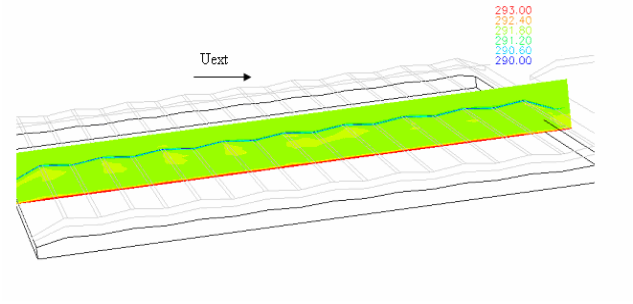

Fig. 18 Simulated thermal field in the centre of the greenhouse (vertical cut in direction of flow)

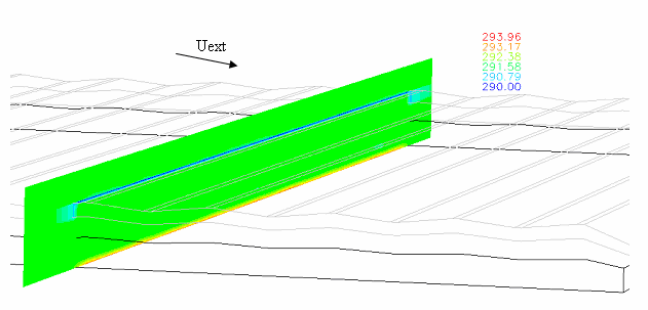

Fig. 19 : Simulated thermal field (K) at the centre of the greenhouse(vertical cut in direction perpendicular to direction of flow)

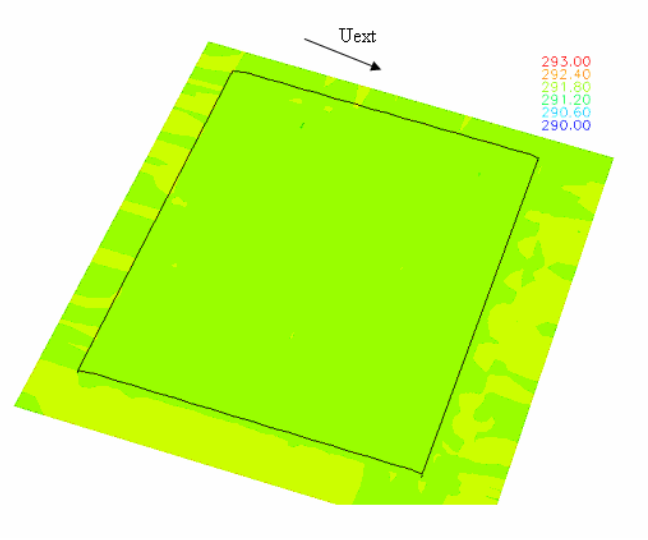

Fig. 20 Champ thermique (K) simulé (coupe horizontale à 1 m au-dessus du sol)

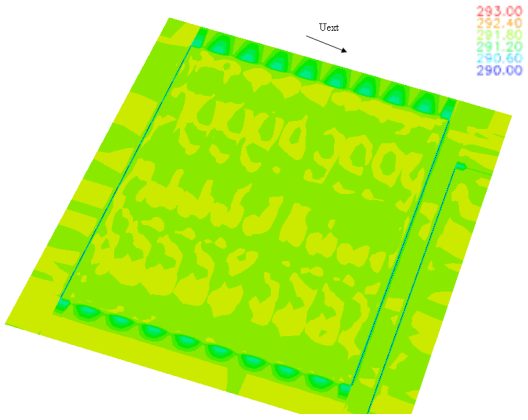

Fig. 21 : Simulated thermal field (K) (horizontal section 4 m above ground level)

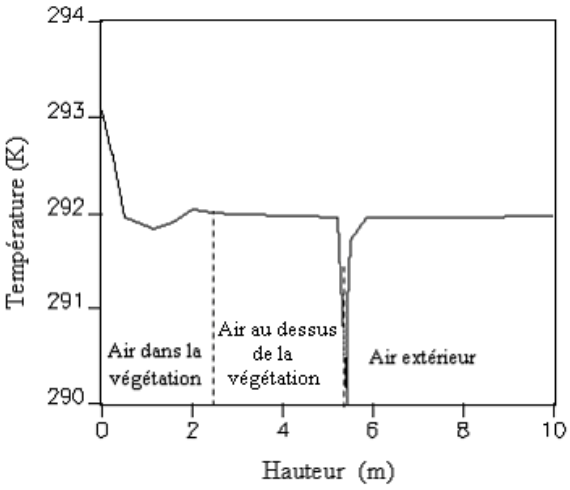

Fig. 22: Vertical temperature profile simulated at the centre of the greenhouse as a function of height

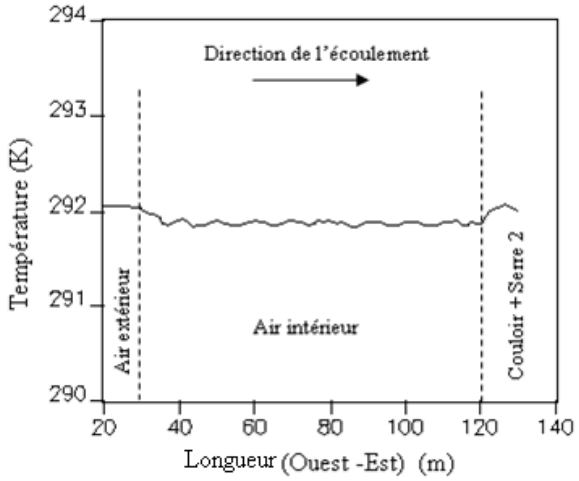

Fig. 23 : Simulated temperature profile 1 m above ground as a function of greenhouse length

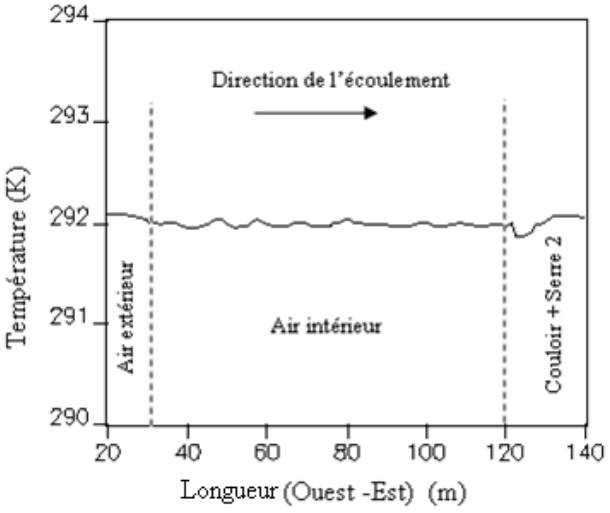

Fig. 24: Simulated temperature profile 3 m above ground as a function of greenhouse length

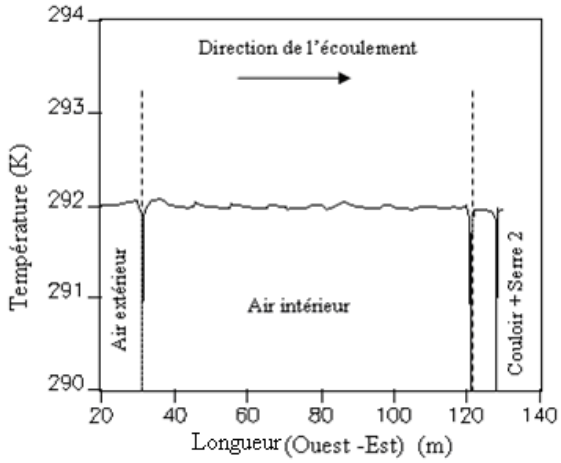

Fig. 25: Temperature profile simulated at 4 m above the ground depending on the length of the greenhouse

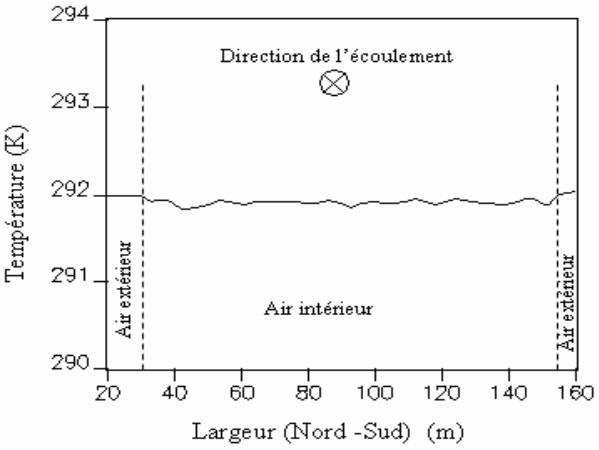

Fig. 26 : Simulated temperature profile at 1 m above ground as a function of greenhouse width

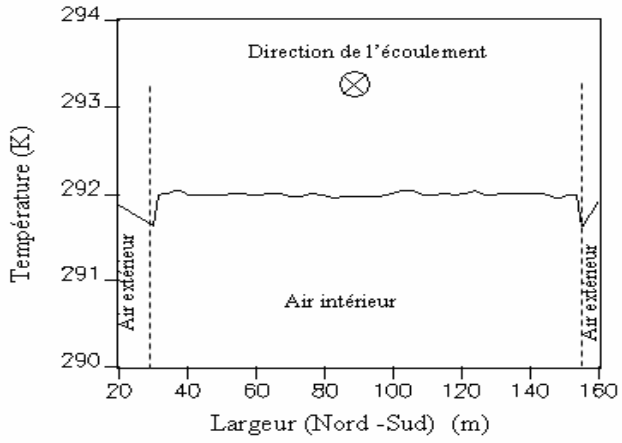

Fig.27 : Simulated temperature profile at 4 m above ground based on greenhouse width

In summary, the simulation of the distribution of thermal fields greenhouse air during the night period,

allows us to conclude that during the night the temperature difference between the inside and outside of the greenhouse is very low and that the air temperature of the greenhouse is slightly higher within the canopy.

5. Conclusion

Numerical simulation is a tool to characterize the thermal and dynamic fields inside the greenhouse. Other parameters such as culture transpiration flow and CO2 concentration could be added to this simulation.

Two approaches were adopted:

-An experimental approach,based on measurements of climatic parameters (temperature) inside and outside the greenhouse, through which we were able to collect the input mathematical models. This approach also allowed us to characterise the internal climate and to understand the natural aeration in the greenhouse and to refine the knowledge of several mechanisms involved.

- A numerical modelling of the greenhouse microclimate using the fluid mechanics code CFD, which allows the prediction of the temperature fields inside the greenhouse after the numerical solution of the Navier-Stockes equations and the heat equation in the considered computational domain.

In general, a significant temperature heterogeneity is observed inside the greenhouse. This phenomenon is mainly due to the geometry of the greenhouse and the alternating arrangement of the ventilation openings on the roof in relation to the direction of the prevailing wind. This arrangement has a remarkable effect on the air circulation within the greenhouse.

In summary, these first results give confidence in the relevance of the numerical simulation of the greenhouse climate and in its concrete use to improve its climatic conditions

One of the most important implications of our study is that farmers can use our work to predict the internal climate changes involved in using the nets or in arranging the crop rows. This allows them to determine the best combination for effective protection against insects.

Nomenclature

K medium permeability (m^2)
U air speed . ($m.s^{-1}$)
Cf non-linear momentum loss coefficient
I_{LA} leaf area index
Q_{sens} convective sensible flux ($W.m^{-2}$)
Q_{lat} latent heat fluxes ($W.m^{-2}$)
T_v canopy temperature (K),
T_i inside air temperatures (K),
C_p specific heat of air at constant pressure ($J.Kg^{-1}.K^{-1}$),
I_{AV} leaf area index,
r_a leaf aerodynamic resistance ($s.m^{-1}$)
d_v characteristic length of the leaf (m);
w_v^* saturated water content of air ($kg.kg^{-1}$)
w_i specific humidity of air ($kg.kg^{-1}$)
r_s tomato leafs tomatal resistance ($s.m^{-1}$)
R_{gi} global radiation inside the greenhouse ($W.m^{-2}$)
R_{ge} Outside radiation ($W.m^{-2}$)
k_c extinction coefficient of radiation,
H total height of canopy(m),
I_{LAS} crop stand leaf area index ($m^2.m^{-2}$)

Greek letters

Φ studied variable
Γ_Φ diffusion coefficient of the quantity Φ
ε dissipation of the turbulent energy.
ρ air density ($kg.m^{-3}$)
μ dynamic viscosity ($kg.s^{-1}.m^{-1}$)
λ air thermal conductivity ($W.m^{-1}.K^{-1}$)
υ air viscosity ($m^2.s^{-1}$)
α the screen porosity

References

[1] El jazouli et al. CFD study of airflow and microclimate patterns inside a multispan greenhouse.*WSEAS transactions on fluid mechanic* DOI :10.37394/232013 (2021) (102-108)

[2] Katsoulas et al Effect of vent openings and insect screens on greenhouse ventilation. *Biosystems Engineering.(2006).01.001*

[3] Hanafi, A et al. Performances of two types of insect screens as a physical barrier against B. tabaci and their impact on TYLCV incidence in a greenhouse tomato in the Souss valley ofMorocco. *Mediterannean Climate.IOBC Bulletin. Vol. 26 (10)(2003) : 39-42.*

[4] Fatnassi, H et al. Optimisation of greenhouse insecte screening with Computational Fluid Dynamics. *Biosystems Engineering 93,(3)(2006), 301- 312.*

[5] Montero et al .Computational Fluid Dynamic modelling of night-time energy fluxes in unheatedgreenhouses.*january.Acta Horticulturae 691 (2005) 403-409.*

[6] Molina-Aiz et al Using computational fluid dynamics tool to model the internal climate of an Almeria-typegreenhouse.*ActaHorticulturae,654, (2004) 271–278.*

[7] Fatnassi et al Optimisation of greenhouse insecte screening with Computational Fluid Dynamics. *Biosystems Engineering 93,(2006) 301- 312.*

[8] Haxaire, R. . Caractérisation et Modélisation des écoulements d'air dans une serre. *Thèse de Docteur en Sciences de l'Ingénieur de l'Université de Nice, Sophia Antipolis. 148p.(1999)*

[9] Demrati,H.etal.Natural ventilation and microclimatic performance of a large scale banana greenhouse. *J.Agri.Engng Res 80 (3): (2001) 291-271.*

[10] Ould Khaoua et al. Modélisation de l'aération naturelle et du microclimat des serres en verre de grande portée sous climat tempéré océanique. *Thèse de Doctorat,Université d'Angers France(2006).*

[11] Demrati,H.et al, Natural ventilation and microclimatic performance of a large scale banana greenhouse. *J.Agri.Engng Res 80 (3): (2001) 291-271.*

[12] Launder and Spalding, The numerical computational of Turbulent flows. *Comp. Method App. Mech. Eng. (1974), 3, 269-289.*

[13] Boulard and Wang. Experimental and numerical study on the heterogeneity of crop transpiration in a plastic tunnel. *Computers & Electronics in Agriculture. 34,(2002) 173–190.*

[14] Bruse, Development of a numerical model for the simulation of exchange processes between small scale environmental design and microclimate in urban areas.*Thèse de Doctorat, University of Bochum.(1998).*

[15] Miguel et al, Airflow through porous screens: from theory to practical considerations. *Energy and Building28 (1998) 63-69.*

[16] Kittas,C.Contribution théorique et expérimentale à l'étude du bilan d'énergie des serres. *Thèse de Doctorat Ingénieur.* (1980)

[17] Kaviany, M.. Principles of heat transfer in porous media. Springer. *Verlaz, Berlin (1995).*